LDV Measurements in Dynamically Separated Flows

M. S. Chandrasekhara[1] and R. D. VanDyken[2]

Navy-NASA Joint Institute of Aeronautics
Department of Aeronautics and Astronautics
Naval Postgraduate School, Monterey, CA 93943, U.S.A.

ABSTRACT

Two component, phase averaged mean velocity data have been obtained with an LDV system, on the upper surface, near the leading edge of an oscillating airfoil undergoing compressible dynamic stall. In particular, the effect of oscillation amplitude has been studied. The results show that at an oscillation amplitude of 10 degrees, a separation bubble forms, that eventually bursts on the upstroke, well beyond the static stall angle. At 2 degrees amplitude, the bubble forms on the upstroke, but dynamic stall occurs on the downstroke. The results reveal new flow physics and the data sets serve as valuable quantitative information for validation of unsteady flow codes at transitional Reynolds numbers. The maximum velocity seen in the flow is about 1.6 times the free stream value and it occurs slightly downstream of the suction peak location. Some of the measurement difficulties are also discussed.

NOMENCLATURE

c	airfoil chord
f	frequency of oscillation, Hz
k	reduced frequency $= \frac{\pi f c}{U_\infty}$
M	free stream Mach number
U,V	velocity components in the x and y directions
U_∞	free stream velocity
$\mathcal{V}$	total velocity, $\sqrt{(U^2+V^2)}$
x,y	chordwise and vertical distance
α	angle of attack
α_0	mean angle of attack
α_m	amplitude of oscillation
ϕ	phase angle of oscillation
ω	circular frequency, radians/sec

1. INTRODUCTION

Dynamic stall is an important problem of interest to the helicopter and fighter aircraft aerodynamicists. The phenomenon relates to the production of high lift by rapidly pitching an airfoil. Its use in practice, however, is limited by the undesirable structural effects induced by the strong pitching moment variation concomitant with the convection of the dynamic stall vortex/vortical structure over the airfoil upper surface. The process if controlled could be used to produce lift coefficients that are twice the normal values. To do so effectively requires a careful and thorough understanding of the process. Basically, the dynamic stall flow is a classic case of forced, unsteady, leading edge separated flow. The leading edge pressure gradient in the flow is $O(1000)$ and thus, the fluid encounters a region of strong adverse pressure immediately following the suction peak, causing it to separate. The local velocity over the airfoil leading edge before separation could reach supersonic values, due to the strong acceleration caused by the large suction peak, even for subsonic free stream Mach numbers. The formation of a shock[1] and its interaction with the local boundary layer adds another dimension to the problem. Additional complications are introduced by the state

[1] *Associate Director and Research Associate Professor;* **Mailing Address: M.S. 260-1 NASA Ames Research Center, Moffett Field, CA 94035-1000, U.S.A.**

[2] *Graduate Student; Currently Research Scientist, Naval Warfare Center, China Lake, CA, 93555*

0-8194-1311-9/93/$6.00

of the airfoil boundary layer and its ability to withstand the generated adverse pressure gradient. Compressibility effects have been known[1,2] to promote stall by reducing the angle of attack for stall inception. The problem is inherently complex and poses significant challenge to both experimentalists and computationalists in their efforts to understand and control it.

As part of a larger study of the problem, the compressibility effects on dynamic stall of oscillating airfoils are being studied at the Navy-NASA Joint Institute of Aeronautics using three nonintrusive optical diagnostic techniques. Since the phenomenon is governed by the airfoil leading edge flow behavior, emphasis was placed on the details of the flow development in this region. The study to be reported, focussed on obtaining the velocity field just around the leading edge of an oscillating airfoil, using a two-component LDV system. The experimental data has been obtained at a Mach number of 0.3, where compressibility effects set in and two amplitudes of oscillation (2 degrees and 10 degrees). A comparison of these results should offer new quantitative information on the effects of amplitude in compressible unsteady separated flow. Also, an especially interesting case of the flow is when the airfoil just reaches an angle of attack close to the static stall angle in its motion and pitches down. The reason for this is it permits study of the formation, growth and possible break down of the separation bubble as the airfoil oscillates. It may provide some clues as to whether the dynamic stall vortex formation occurs during the bursting process of the bubble or not.

2. DETAILS OF THE EXPERIMENT

2.1. The facility

The experiments were carried out in the Compressible Dynamic Stall Facility (CDSF) at the Fluid Mechanics Laboratory of NASA Ames Research Center. The CDSF is an indraft wind tunnel with a 0.25m X 0.35m test section and is equipped with a drive for producing a sinusoidal variation of the airfoil angle of attack. The flow in the tunnel is controlled by a choked, variable area downstream-throat, to produce a Mach number range of $0 \leq M \leq 0.5$. The flow is produced by a 6MW, $108m^3/s$, continuous running evacuation compressor. The airfoil mean angle of attack, α, can be set to $0 \leq \alpha \leq 15^0$, the amplitude of oscillation, α_m, to $2^0 \leq \alpha_m \leq 10^0$, and the oscillation frequency, f, to $0 \leq f \leq 100Hz$. Fig. 1[3] shows a schematic of the drive system. More details are given in Ref. 3.

2.2. LDV technique in dynamic stall flows

A two-color, two-component, frequency-shifted, Argon-Ion laser based, off-axis, forward scatter TSI system was used for velocity measurements. Traversing was accomplished by directing the 4 beams on to a 0.352m focal length lens mounted on a computer controlled traverse. Fig. 2[3] presents a schematic of the CDSF instrumentation. The signals were processed by TSI 1990 counters. $1\mu m$ polystyrene latex particles suspended in alcohol injected from the tunnel inlet were used for seeding. Special phase locking circuitry enabled handling of the random LDV data and the unsteady position data. The LDV data was acquired in the coincidence mode with the window width arbitrarily set to $50\mu sec$. The coincidence pulse was used to trigger data acquisition and freeze the rapidly changing encoder values till data transfer to the computer could be completed as shown in Fig. 3. The randomness of the LV data and the need to record the appropriate phase angle when a coincident sample appeared demanded the use of the inverse method described in the figure. The data acquisition and processing software incorporated the standard tests of data validation, phase averaging by binning the data appropriately, identifying holes in the data if the number of samples in any bin was less than a preselected value (50 in this case) and providing phase distributions of the velocity components. Any time the standard criteria were not satisfied, the data set was rejected and a new set was acquired. A minimum of 10,000 samples were collected per channel at each measurement point. The complete details of the scheme could be found in Chandrasekhara and Ahmed[4].

2.3. Experimental conditions

As stated earlier, the flow Mach number was set to 0.3, corresponding to a Reynolds number of 540,000. The oscillation frequency was 21.6Hz, and the reduced frequency of 0.05. The airfoil section was NACA 0012 with 0.0762m chord and was oscillated about the 25% chord point. The amplitudes of oscillation were 10 degrees and 2 degrees.

For the former, the airfoil angle of attack varied as

$$\alpha = 10^0 - 10^0 \sin \omega t$$

Thus, phase angle, $\omega t = 0^0$ corresponded to $\alpha = 10^0$, 90^0 to $\alpha = 0^0$ on its downstroke, 180^0 to $\alpha = 10^0$ on the upstroke and 270^0 to the maximum angle of attack of 20^0. For the case of 2 degrees amplitude, the variation in angle of attack was between 8 - 12 degrees. The LDV probe volume was traversed in the range $-0.167 \leq \frac{x}{c} \leq .167$ and $0.083 \leq \frac{y}{c} \leq 0.167$, with x and y measured from the airfoil leading edge at zero degrees angle of attack.

3. RESULTS AND DISCUSSION

Due to limitation of space, only sample results typical of the flow are presented below. First, the variations of velocity with phase angle are discussed. Subsequently, velocity profiles and vorticity plots are analyzed.

3.1. Phase distribution of velocity

Fig. 4a shows the variation of the streamwise velocity U, with phase angle at x/c = 0.067 for $\alpha = 10^0 - 10^0 \sin \omega t$. Dramatic changes can be seen in the phase plots at y/c locations close to the airfoil surface. At y/c = 0.083 during the downstroke, the velocity decreases to $1.05U_\infty$ at $\phi = 90^0$, $\alpha = 0^0$; and begins to increase as expected during the upstroke of the airfoil. This is true for fluid layers at other heights as well. However, at $\phi = 155^0$, $\alpha = 5.5^0$, the velocity drops rapidly to $0.4U_\infty$ over $155^0 \leq \phi \leq 202^0$, corresponding to $5.5^0 \leq \alpha \leq 13.7^0$. Such a drop can be attributed to the presence of a separation bubble that penetrates the LDV probe volume as the airfoil pitches up. Eventually at this location, the airfoil blocks off the beams and thus no data could be obtained until a phase angle of $\approx 330^0$. (This is the reason for the gaps in the distribution seen for some phase angles.) At the higher locations, the phase angle range over which this drop occurs decreases since the bubble is narrow at the top. Fig. 4a shows further that the bubble bursts between $\phi = 200^0 - 216^0$. Measurements of the V component of velocity presented in Fig. 4b also show rapid increases in this phase angle range. In these figures, all measurement points below y/c = 0.117 are within the separation bubble and the phase variation seen at y/c = 0.133 is typical of all other outer points in the flow. The vertical velocity in the bubble is generally small, $O(0.1U_\infty)$. In steady flow leading edge type stall, bubble bursting is a rapid event. However, in the unsteady dynamic stall flow, it occurs over a range of phase angles. Fig. 4b shows a gradually increasing V velocity until $\phi = 216^0, \alpha = 15.9^0$, which is known to be the dynamic stall angle from the earlier schlieren studies[2]. (The static stall angle for this Mach number is 12.4 degrees). At this angle of attack, the dynamic stall vortex is shed and the airfoil shear layer detaches from the surface everywhere, except at the leading edge. This causes a large V velocity and concurrently, the U velocity drops. These features are distinctly seen in Fig. 4a and 4b. Similar plots were obtained for the 2 degree amplitude case, which also showed the separation bubble. However, its bursting could not be so clearly established.

3.2. Velocity profiles in a cycle

Fig. 5 shows[5] the range of total velocity profiles for the upstroke portion of the oscillation cycle at x/c = 0.083 for an amplitude of 10 degrees. At a low angle of attack of 6.9^0 on the upstroke, the mean velocity shows a point of inflection through the bubble at y/c = 0.1. The local velocity is about $1.35U_\infty$. The inflection point moves outwards as the airfoil pitches up, because the bubble grows during the process. Correspondingly, at the same y/c location, lower velocities are measured. (As stated in Sec. 2.3, line y/c = 0 corresponds to the airfoil chord line at $\alpha = 0^0$). The bubble causes the drop seen at the lower locations. However, it should be noted that in this and other profiles, whereas the velocities dropped to as low as $0.4U_\infty$, no negative streamwise velocities were encountered. This is believed to be due to the fact that in dynamic stall flow, the region of negative velocity is very small, $O(0.01c)$; it was difficult to seed the flow locally and also obtain optical access to the boundary layer, as its thickness was about one probe volume diameter. The incidental blockage of the beams during parts of the oscillation cycle was responsible for loss of the signal at different phase angles depending on the instantaneous height of the measurement volume above the airfoil. Despite all these problems, the trends seen are consistent. As dynamic stall occurs at 15.9^0, the velocity profile changes to an inverted 'S' shape. The flow develops unusual shear patterns in this state. At post-stall phase angles, the velocities are still large.

Fig. 6a and 6b show the streamwise velocity profiles at x/c = 0.033 and x/c = 0 .083 for $\alpha = 10^0 - 2^0 \sin \omega t$. In Fig. 6a, large velocity variations and hence shear are present at x/c = 0.033. The location of the peak velocity

moves into the outer layers farther from the airfoil surface as it pitches from $\alpha = 8^0 - 12^0$ and moves towards it on the downstroke. The profiles become steeper as the lower velocity locations closer to the airfoil are encountered, as evidenced by the velocity range of $0.8U_\infty - 1.4U_\infty$ at $\alpha = 12^0$ and $1.2U_\infty - 1.4U_\infty$ at $\alpha = 8^0$. Since no drastic changes in the curvature of the profiles are seen, the profiles lead one to conclude that the bubble does not burst at this location. In comparison, Fig. 6b for x/c = 0.083 offers nearly the same picture on the upstroke. However, inflection and nearly inverted 'S' shaped distributions appear near the top of the cycle, which disappears again at $\alpha = 10.68^0$ on the downstroke. This suggests a partial breakdown of the bubble. Recently obtained interferometry data has shown that the flow remains fully attached throughout the upstroke, but separates mildly on the downstroke during a small angle of attack range. The distinct differences seen at $\alpha = 10.68^0$ on the upstroke and downstroke shows that hysteresis is present in even this low amplitude unsteady flow.

3.3. Contours of z-component of vorticity

The z-component of vorticity normalized by $\frac{c}{U_\infty}$ is presented in Fig. 7 and Fig. 8. The distributions were obtained by interpolating the velocity component data using a monotonic spline curve fit and calculating the gradients from the fitted curve and also separately from the raw processed data using PLOT3D package. But the latter were not as smooth as those shown in the figures. There could be substantial noise in the data due to the interpolation and numerical differentiation used. Since this is common to all of the distributions discussed a comparison is still valid. The uncertainty in the data is estimated to be about 20%.

Fig. 7 compares the leading edge vorticity field at $\alpha = 10^0$ on the upstroke for the two amplitudes under discussion. Fig. 7a drawn for an amplitude of 2 degrees shows that the peak vorticity level is ≈ -30 units (clockwise) and occurs very near the leading edge at y/c = 0.08. Much of the flow contains only clockwise vorticity only (contour levels 3 - 8) between x/c = 0 to x/c = 0.15. This is to be expected since clockwise vorticity is added by the pitch-up motion. Isolated small pockets of anticlockwise vorticity at a low level (of about 10 units) are also present. At an amplitude of 10 degrees in Fig. 7b, a significantly higher clockwise vorticity of -60 units is seen which can be attributed to the larger amplitude of oscillation and hence, a greater input of clockwise vorticity through the surface motion. Of greater interest is that it is contained in structures located at around x/c = 0.1, y/c = 0.08. Just above the leading edge, the vorticity levels are zero, although the airfoil is still pitching-up. It is believed that at the leading edge itself, clockwise vorticity is still being added and hence present, but it has begun to be convected over the surface. The large levels of the vorticity and the structures observed point to the fact that the vorticity has begun to coalesce.

Fig. 8a and 8b show the vorticity contours for $\alpha = 10^0 - 2^0 \sin\omega t$ for angles of attack of 11.53 degrees and 11 degrees. In Fig. 8a, the vorticity level has exceeded -40 units and is contained in a structure very close to the leading edge. The region of vorticity level of -10 units extends to x/c = 0.15 and y/c = 0.1 in a large structure seemingly attached to the leading edge. Fig. 8b shows that at 11.0 degrees angle of attack, the peak level has dropped to -25 units and the region of clockwise vorticity is much smaller than seen in Fig. 8a. Since the peak vorticity level was found to increase again at $\alpha = 10^0$(distribution not shown), it is clear that the vorticity is partially shed some where between $\alpha = 11.53^0 - 11^0$. This points to mild stall occurring on the downstroke. A comparison with the 10 degrees amplitude case showed that vorticity levels dropped by as much as 40% once stall occurred. As reattachment and flow development occurred, the levels began to increase again.

4. CONCLUDING REMARKS

Typical results of laser velocimetry measurements and vorticity field over an airfoil oscillating in compressible separated flow have been discussed. The study points to the following conclusions.

1. Dynamic stall occurs as the separation bubble bursts and the leading edge vorticity is shed over a small range of angles of attack. For the two degrees amplitude case, this happens on the downstroke, *below* the static stall angle.

2. Velocity profiles show a wide variation through the cycle. The maximum velocity reaches $1.6U_\infty$.

3. The vorticity data shows that the more than twice the vorticity could be added to the flow by the large amplitude oscillatory motion.

5. ACKNOWLEDGEMENTS

The work was supported by the U.S. Army Research Office under grants MIPR-114-91 and MIPR-130-92 to the U.S. Naval postgraduate School. Additional support was received from the U.S. Air Force of Scientific Research MIPR-92-0004. The work was performed in the Fluid Mechanics Laboratory Branch of the NASA Ames Research Center. The authors acknowledge the support of the agencies.

6. REFERENCES

1. Chandrasekhara, M.S. and Brydges, B.E. "Amplitude Effects on Dynamic Stall of an Oscillating Airfoil", *AIAA Paper 90-0575*, Jan. 1990.

2. Chandrasekhara, M.S. and Carr, L.W. "Flow Visualization Studies of the Mach Number Effects on the Dynamic Stall of Oscillating Airfoils", *Jl. of Aircraft*, Vol. 27, No. 6, pp. 516-522, June 1990.

3. Carr, L.W. and Chandrasekhara, M.S., "Design and Development of a Compressible Dynamic Stall Facility", *Jl. of Aircraft*, Vol. 29, No. 3, pp. 314-318, June 1992.

4. Chandrasekhara, M.S., and Ahmed, S., "Laser Velocimetry Measurements of Oscillating Airfoil Dynamic Stall Field", *AIAA Paper 91-1799*, June 1991.

5. Chandrasekhara, M.S., and VanDyken, R.D., "Oscillating Airfoil Velocity Field During Large Amplitude Dynamic Stall", *Proc. 8th Symposium on Turbulent Shear Flows*, Vol. 2, pp. I-3 - I-4, Münich, Germany, Sept. 9-11, 1991.

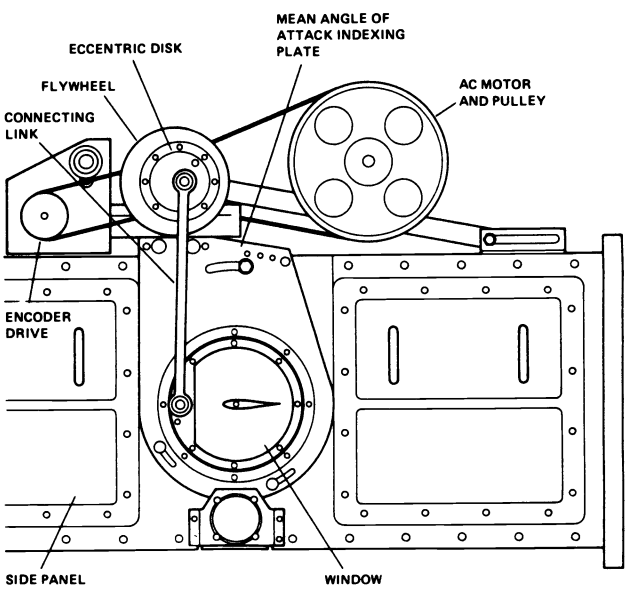

Fig. 1. Side-view of the Compressible Dynamic Stall Facility.

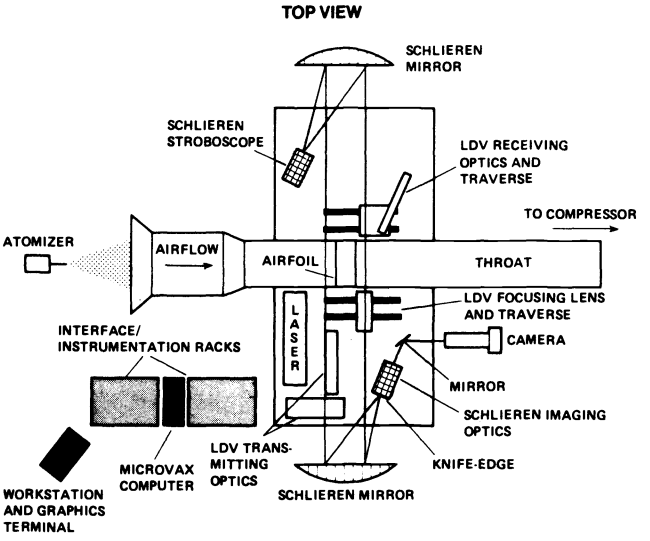

Fig. 2. Schematic of the LDV System in Use in the CDSF.

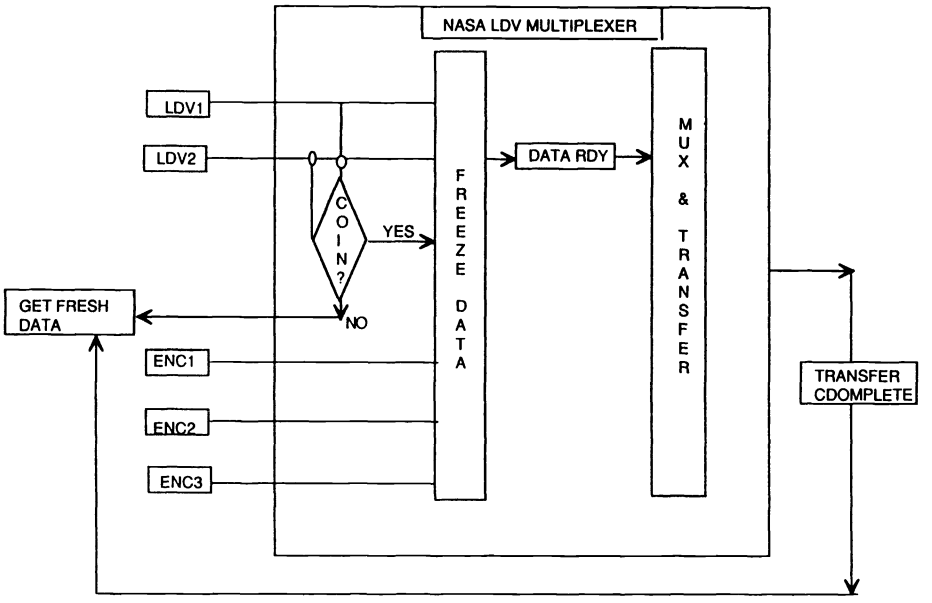

Fig. 3. Schematic of the Unsteady Flow LDV Data Acquisition Method.

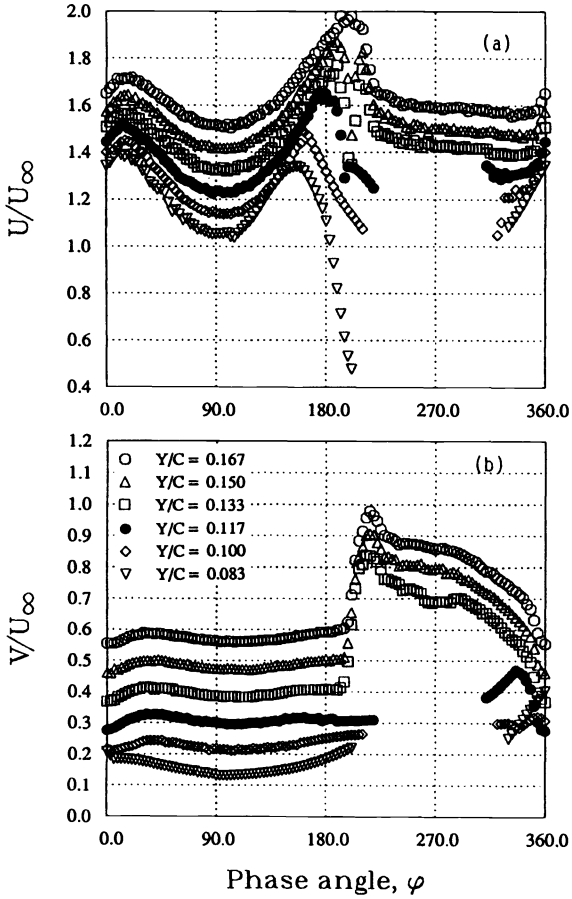

Fig. 4. Phase Distribution of Velocity, $\alpha = 10^0 - 10^0 \sin \omega t$, x/c = 0.067. (Velocities offset by $0.1U_\infty$ at each station). (a) Streamwise Component, U; (b) Vertical Component, V.

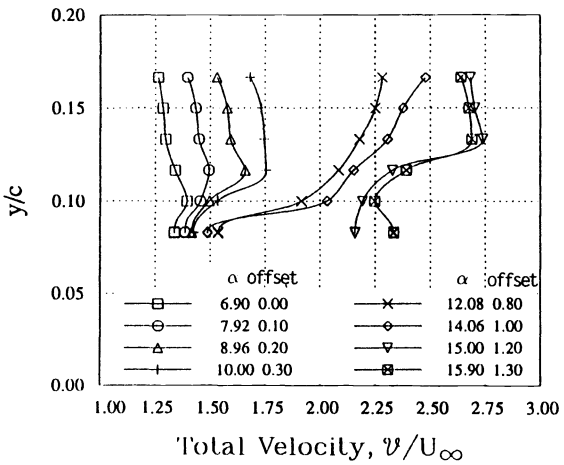

Fig. 5. Variation of Total Velocity,$\mathcal{V}$ During Upstroke; $\alpha = 10^0 - 10^0 \sin \omega t$; x/c = 0.083. (Velocity offset as indicated).

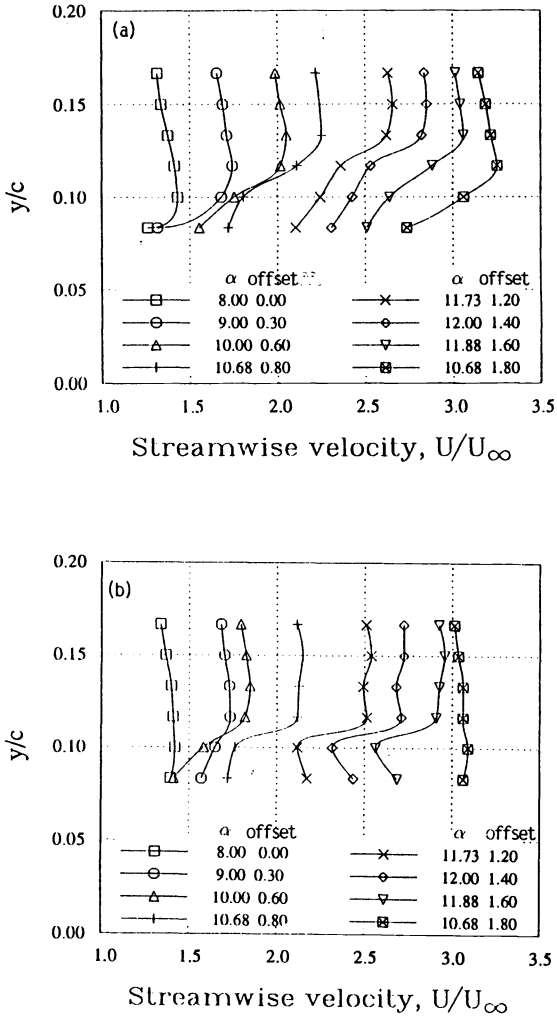

Fig. 6. Variation of Streamwise Velocity, U in an Oscillation Cycle; $\alpha = 10^0 - 2^0 \sin \omega t$. (Velocity offset as indicated). (a) x/c = 0.033; (b) x/c = 0.083.

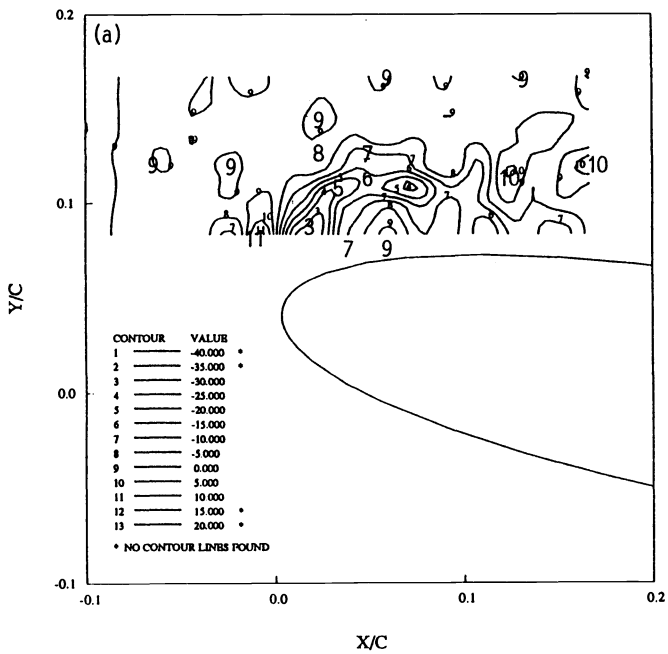

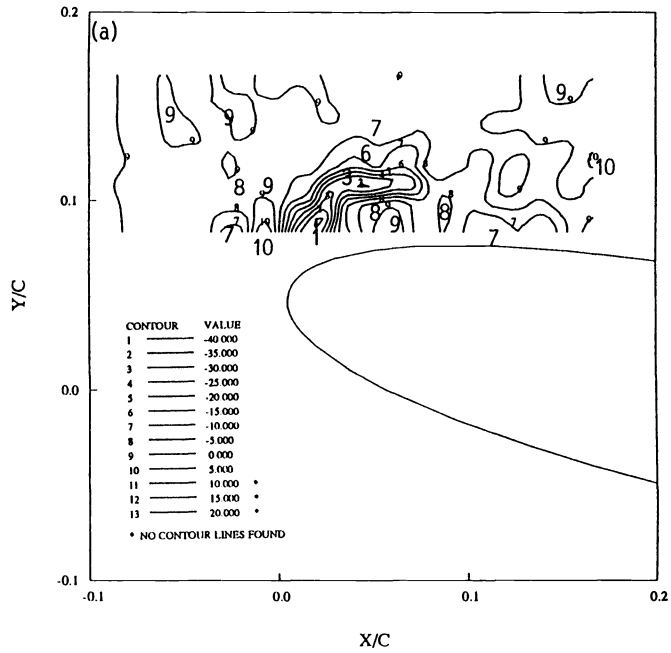

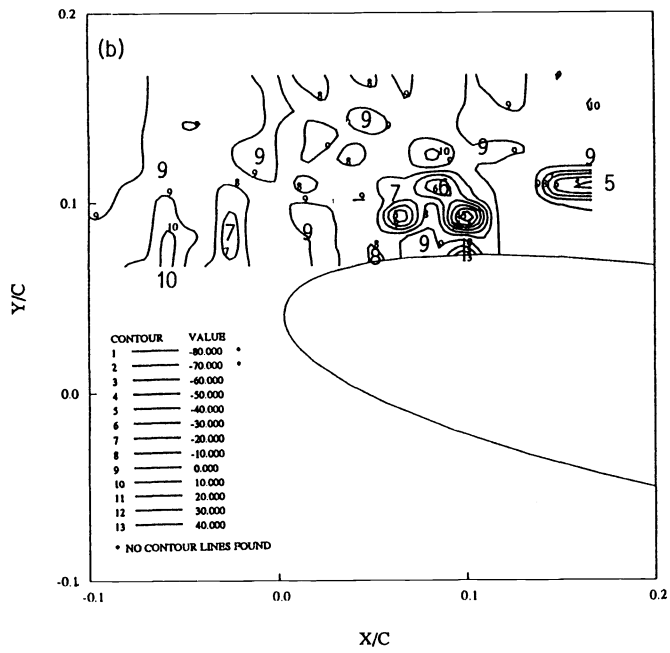

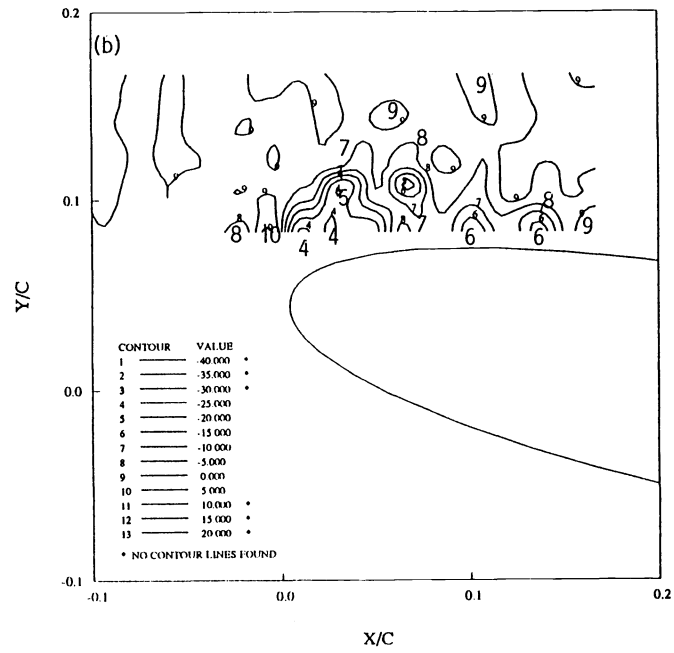

Fig. 7. Contours of Z-component of Vorticity, $\phi = 180^0$ $\alpha = 10^0$, Upstroke. (a) $\alpha = 10^0 - 2^0 \sin \omega t$; (b) $\alpha = 10^0 - 10^0 \sin \omega t$.

Fig. 8. Contours of Z-component of Vorticity During the Airfoil Downstroke, $\alpha = 10^0 - 2^0 \sin \omega t$. (a)$\alpha = 11.53^0$; (b) $\alpha = 11^0$